

Surface Engineering with Poly(ethylene glycol) Photolithography to Create High-Density Cell Arrays on Glass

Alexander Revzin, Ronald G. Tompkins, and Mehmet Toner*

Center for Engineering in Medicine and Surgical Services, Massachusetts General Hospital, Harvard Medical School, and Shriners Hospital for Children, Boston, Massachusetts 02114

Received June 25, 2003. In Final Form: August 14, 2003

This manuscript presents a microfabrication-derived approach for controlling mammalian cell–surface interactions. Poly(ethylene glycol)-diacrylate (PEG-DA) was patterned, in a process analogous to photolithography, to manufacture high-density arrays of micrometer-scale PEG hydrogel wells on glass. Individual wells consisted of PEG walls and glass attachment pads; thus, as a result of the biological inertness of PEG, microwell patterning created a highly ordered biointerface with modulating-cell or protein-repellent properties. Fabricated hydrogel microstructures proved very effective in guiding and confining adhesion of transformed 3T3 fibroblasts and primary rat hepatocytes to defined regions on the glass substrate. PEG-patterned glass surfaces were selectively modified with collagen (type I) to induce hepatocyte attachment. Localization of the fluorescein-conjugated collagen within the glass attachment pads of PEG hydrogel microwells was visualized by fluorescence microscopy. Further surface analysis was performed by tapping mode atomic force microscopy conducted within individual PEG wells. Protein-modified regions inside the wells had a root-mean-square roughness of 1.13 ± 0.03 nm compared to 0.7 ± 0.04 nm for alkylsilane-treated regions lacking protein. The cell occupancy of $96.7 \pm 1.9\%$ within the arrays of $30 \times 30 \mu\text{m}$ individual wells was demonstrated for 3T3 fibroblasts. At the same time, cells remained effectively isolated in the individual PEG microwells. Primary hepatocytes attached and became fully confluent within the collagen-coated PEG after 24 h of incubation. Each $30 \times 30 \mu\text{m}$ well contained one to three hepatocytes. Cells patterned on the surface remained viable after 24 h of incubation.

Introduction

The ability to engineer cell–surface interactions and to exercise spatial control over cells is essential for in vitro simulations of physiologically relevant scenarios. These in vitro experimental models will lead to a better understanding of organ function and enable tissue engineering of bioartificial systems that mimic natural organs more closely.¹ In addition, the advent of intracellular reporter molecules (e.g., green fluorescence protein) and sensitive microscopy instrumentation provide the tools for rapid and quantitative intracellular determination of biological activity. Thus, high-density arrays of genetically engineered live cells may serve as bioassays for high-throughput screening of drug candidates or provide molecular biology information pertaining to the dynamics of gene expression.² Phenotyping of the arrayed cells based on the morphological characteristics may also prove valuable for clinical diagnostic purposes. Finally, rendering surfaces resistant to cell attachment is necessary for the creation of a controlled biointerface between the cellular and the microfabricated components of biological microdevices and for the prevention of biofouling in these devices.³

A number of cellular micropatterning techniques have been reviewed in the literature.^{4,5} While methods utilizing

elastomeric stencils^{6,7} or microfluidic channels^{8,9} enabled cell patterning with minimal surface engineering, the majority of the reports detail designing the biointerface for cell–surface interactions. Bhatia et al. employed photoresist technology to define cell-adhesive collagen islands and demonstrated preferential attachment of hepatocytes to these adhesion sites.^{10,11} This method led to the co-cultivation of hepatocytes and fibroblasts and helped to elucidate effects of homotypic and heterotypic cell–cell interactions on hepatic function. Others reported the use of deep UV photolithography of chemisorbed alkylsilanes to create substrata with differential cytophobic/cytophilic properties.^{12,13} This technology enabled guidance of neuronal adhesion and neurite outgrowth.

The cellular patterning strategies described above were tailored specifically for the cellular system of interest, for example, affinity of primary hepatocytes toward a collagen-presenting substrate. To design surfaces resistant

(5) Folch, A.; Toner, M. *Annu. Rev. Biomed. Eng.* **2000**, *2*, 227.

(6) Folch, A.; Jo, B.-H.; Hurtado, O.; Beebe, D. J.; Toner, M. *J. Biomed. Mater. Res.* **2000**, *52*, 346–353.

(7) Ostuni, E.; Kane, R.; Chen, C. S.; Ingber, D. E.; Whitesides, G. M. *Langmuir* **2000**, *16*, 7811–7819.

(8) Chui, D. T.; Jeon, N. L.; Huang, S.; Kane, R. S.; Wargo, C. J.; Choi, I. S.; Ingber, D. E.; Whitesides, G. M. *Proc. Natl. Acad. Sci. U.S.A.* **2000**, *97*, 2408–2413.

(9) Takayama, S.; McDonald, J. C.; Ostuni, E.; Liang, M. N.; Kenis, P. J. A.; Ismagilov, R. F.; Whitesides, G. M. *Proc. Natl. Acad. Sci. U.S.A.* **1999**, *96*, 5545–5548.

(10) Bhatia, S. N.; Balis, U. J.; Yarmush, M. L.; Toner, M. *Biotechnol. Prog.* **1998**, *14*, 378–387.

(11) Bhatia, S. N.; Yarmush, M. L.; Toner, M. *J. Biomed. Mater. Res.* **1997**, *34*, 189–199.

(12) Dulcey, C. S.; Georger, J. H.; Krauthamer, V.; Stenger, D. A.; Fare, T. L.; Calvert, J. M. *Science* **1991**, *252*, 551–554.

(13) Ravenscroft, M. S.; Bateman, K. E.; Shaffer, K. M.; Schessler, H. M.; Jung, D. R.; Schneider, T. W.; Montgomery, C. B.; Custer, T. L.; Schaffner, A. E.; Liu, Q. A.; Li, X.; Barker, J. L.; Hickman, J. J. *J. Am. Chem. Soc.* **1998**, *120*, 1269–1277.

* Corresponding author. Address: Shriners Hospital for Children, 51 Blossom St., Boston, MA, 02114. Phone: (617) 371-4883. Fax: (617) 371-4950. E-mail: mtoner@sbi.org.

(1) Patrick, C. W. J.; Mikos, A. G.; McIntire, L. V., Eds.; *Frontiers in Tissue Engineering*; Pergamon Press: New York, 1998.

(2) Scheirer, W. *High Throughput Screening: The Discovery of Bioactive Substances*; Marcel Dekker, Inc.: New York, 1997.

(3) Voldman, J.; Gray, M. L.; Schmidt, M. A. *Annu. Rev. Biomed. Eng.* **1999**, *1*, 401–425.

(4) Whitesides, G. M.; Ostuni, E.; Takayama, S.; Jiang, X.; Ingber, D. E. *Annu. Rev. Biomed. Eng.* **2001**, *3*, 335–373.

to attachment of a wide range of biomolecules, poly(ethylene glycol) (PEG) grafting is commonly employed.^{14–18} The biological inertness of PEG is attributed to its hydrophilicity and charge neutrality.¹⁹ Self-assembly of PEG-terminated alkanethiols on gold combined with microcontact printing²⁰ enabled studies pertaining to the effect of the cell shape on cell function in the primary hepatocytes²¹ and the onset of apoptosis in the capillary endothelial cells.²² Healy and co-workers employed a multistep surface modification process that included photoresist lithography followed by selective grafting of a PEG-containing interpenetrating network on glass. Surfaces micropatterned in this manner were employed to investigate the interdependence between the projected cell area and the function of osteoblasts.²³ This method has recently been amended by replacing the photolithography step with selective oxygen plasma etching to define cell-adhesive or cell-repellent regions of glass.²⁴ Self-assembly of PEG-terminated silanes on glass has also been employed for cell patterning.²⁵ Other strategies included selective surface grafting of PEG-terminated hyperbranched polymer films on gold and demonstrated patterning of mammalian and bacterial cells.^{26,27}

Recently, a novel PEG surface modification and patterning process has been proposed.^{28,29} This approach mimics traditional photolithography in that spin-coating and UV exposure through a photomask are employed to create a polymer pattern. However, rather than form a barrier to penetration of etching agents, PEG hydrogel microstructures resist protein or cell adhesion.³⁰ While the majority of micropatterning techniques modify surfaces from the “bottom-up”, PEG patterning employed in the present study is a “top-down” process. Thus, a cell- or protein-repellent material can be spin-coated directly onto the substrate, photopatterned, and developed in water, ensuring simplicity of the process and minimizing cytotoxicity. This PEG microfabrication method proved amenable to the patterning of encapsulated, living mammalian cells.³¹ In addition, initial results demonstrated the utility of this surface patterning approach for controlling mammalian and bacterial cell attachment.³⁰

This present work demonstrates high-density mammalian cell patterning on PEG hydrogel-modified glass substrates. Murine 3T3 fibroblasts and primary rat hepatocytes were patterned within 80 × 80 arrays of wells with 30 × 30 μm individual dimensions. PEG microwells were selectively modified with collagen (type I) to enable attachment of primary hepatocytes. Fluorescence microscopy and tapping-mode (TP) atomic force microscopy (AFM) were employed to verify and analyze the protein deposition into the microwells. Evidence of high-density patterning of both fibroblasts and hepatocytes on glass was obtained by optical and electron microscopies. Single fibroblasts were reproducibly isolated inside 900-μm² PEG wells, while one to three hepatocytes were typically present within wells of the same dimensions. Micropatterned hepatocytes and fibroblasts remained viable after 24 and 12 h of incubation, respectively, as verified by Live/Dead staining.

Experimental Section

Materials. Poly(ethylene glycol) diacrylate (PEG-DA; MW 575), 2,2'-dimethoxy-2-phenylacetophenone (DMPA), anhydrous toluene, ethanol, the desiccator, and the glovebag were purchased from Aldrich Chemical Co. (Milwaukee, WI). The silane adhesion promoters, 3-acryloxypropyl trichlorosilane (**1**) and 3-(*n*-allylamino)propyl trimethoxysilane (**2**), were purchased from Gelest, Inc. (Morrisville, PA). Sulfuric acid and hydrogen peroxide were obtained from J. T. Baker (Phillipsburg, NJ). Glass slides (75 × 25 mm), tissue culture flasks, and serological pipets were obtained from Fisher Scientific (Fair Lawn, NJ). Phosphate buffered saline (PBS) 1×, Dulbecco's Modified Eagle's Medium (DMEM) with 25 mM glucose and 4 mM glutamine, penicillin, streptomycin, trypan blue, and trypsin were purchased from Gibco (Gaithersburg, MD). Bovine calf serum was purchased from JRH Biosciences (Lenexa, KS). The Live/Dead viability/cytotoxicity kit and fluorescein-conjugated collagen (type I from bovine skin) were obtained from Molecular Probes (Eugene, OR). Murine 3T3 fibroblasts were purchased from American Type Culture Collection (Manassas, VA). Female Lewis rats (Charles River Laboratories, Wilmington, MA) were used as a source of hepatocytes. Details of the procedure for isolation of hepatocytes are described elsewhere.³²

Silane Modification of Glass Substrates. The glass slides were scrupulously cleaned prior to silane assembly. The slides were immersed for 30 min in “piranha” solution consisting of a 3:1 ratio of aqueous solutions of 50% (v/v) sulfuric acid and 30% (w/v) hydrogen peroxide (*caution: this mixture reacts violently with organic materials and must be handled with extreme care*). After removal from the “piranha” bath, glass slides were thoroughly rinsed with deionized (DI) water and dried under nitrogen. Clean slides were stored at room temperature in the Class 1000 clean room. Immediately prior to silane modification, slides were placed in an oxygen plasma chamber (PX-250, March Instruments, Inc., Concord, CA) for 3 min at 150 mW and 50% oxygen. This step ensured the presence of the hydroxyl groups needed for silane self-assembly. Surface modification with chlorosilane adhesion promoter **1** was achieved by immersing glass slides in a 2 mM solution of **1** in anhydrous toluene for 30 min. Functionalization of glass substrates with alkoxysilane agent **2** was accomplished by immersing glass slides into a 4% (v/v) solution of **2** in anhydrous toluene for 1 h. After removal from the silane solution, slides were rinsed in toluene and dried with nitrogen. Both the solution preparation and the silane self-assembly reaction were conducted under a nitrogen atmosphere in a glovebag, at room temperature. The silanized glass slides were stored under a vacuum in a desiccator.

Fabrication of Hydrogel Micropatterns. Figure 1 illustrates the process flow for the fabrication of PEG hydrogel micropatterns. PEG hydrogel patterns were fabricated from the precursor solution of PEG-DA (MW 575) with 1% (w/v) photoinitiator, DMPA. This solution was spun at 1000 rpm for 6 s onto the silane-treated glass surface containing terminal acrylate or

(14) Merrill, E. W.; Salzman, E. W. *ASAIO J.* **1983**, *6*, 60–66.

(15) Prime, K.; Whitesides, G. *Science* **1991**, *1164*–1167.

(16) Prime, K. L.; Whitesides, G. M. *J. Am. Chem. Soc.* **1993**, *115*, 10714–10721.

(17) Lee, S.-W.; Laibinis, P. E. *Biomaterials* **1998**, *19*, 1669–1675.

(18) Malmsten, M.; Emoto, K.; Van Alstine, J. M. *J. Colloid Interface Sci.* **1998**, *202*, 507–517.

(19) Sofia, S. J.; Merrill, E.; Harris, J. M. a.; Zalipsky, S., Ed.; *Poly(ethylene glycol): chemistry and biological applications*; American Chemical Society: Washington, DC, 1997; Vol. 680, pp 342–360.

(20) Xia, Y.; Whitesides, G. M. *Angew. Chem., Int. Ed.* **1998**, *37*, 550–575.

(21) Singhvi, R.; Kumar, A.; Lopez, G. P.; Stephanopoulos, G. N.; Wang, D. I. C.; Whitesides, G. M.; Ingber, D. E. *Science* **1994**, *264*, 696–698.

(22) Chen, C. S.; Mrksich, M.; Huang, S.; Whitesides, G. M.; Ingber, D. E. *Science* **1997**, *276*, 1425–1428.

(23) Thomas, C. H.; Lhoest, J. B.; Castner, D. G.; McFarland, C. D.; Healy, K. E. *J. Biomech. Eng.* **1999**, *121*, 40.

(24) Tourovskaia, A.; Barber, T.; Wickes, B. T.; Hirdes, D.; Grin, B.; Castner, D. G.; Healy, K. E.; Folch, A. *Langmuir* **2003**, *19*, 4754–4764.

(25) Irimia, D.; Karlsson, J. O. M. *Biophys. J.* **2002**, *82*, 1858–1868.

(26) Amirpour, M. L.; Gosh, P.; Lackowski, W. M.; Crooks, R. M.; Pishko, M. V. *Anal. Chem.* **2001**, *73*, 1560–1566.

(27) Rowan, B.; Wheeler, M. A.; Crooks, R. M. *Langmuir* **2002**, *18*, 9914–9917.

(28) Revzin, A.; Russell, R. J.; Yadavalli, V. K.; Koh, W.-G.; Deister, C.; Hile, D. D.; Mellott, M. B.; Pishko, M. V. *Langmuir* **2001**, *17*, 5440–5447.

(29) Ward, J. H.; Bashir, R.; Peppas, N. A. *J. Biomed. Mater. Res.* **2001**, *56*, 351–360.

(30) Koh, W. G.; Revzin, A.; Simonian, A.; Reeves, T.; Pishko, M. *Biomed. Microdevices* **2003**, *5*, 11–19.

(31) Koh, W.-G.; Revzin, A.; Pishko, M. V. *Langmuir* **2002**, *18*, 2459–2462.

(32) Dunn, J. C. Y.; Yarmush, M. L.; Koebe, H. G.; Tompkins, R. G. *FASEB J.* **1989**, *3*, 174–179.

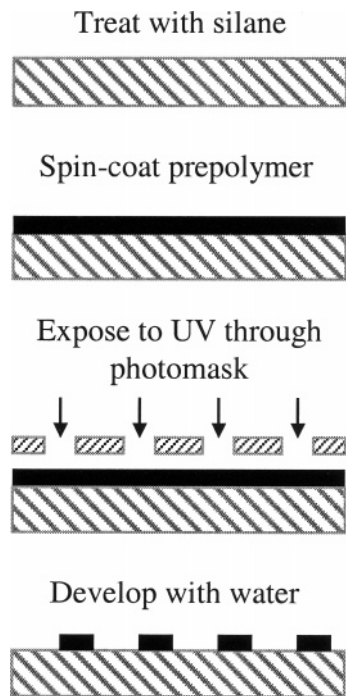


Figure 1. Process flow for the fabrication of PEG hydrogel microstructures.

vinyl functional groups using a spin-coater (Machine World, Inc., Redding, CA). The uniform layer of the PEG-DA precursor solution on glass was then exposed through a chrome/soda lime photomask (Advance Reproductions, North Andover, MA) to 365-nm, 15-mW/cm² UV light from a Q 2001 mask aligner (Quintel Co., San Jose, CA). The exposure times ranged from 1 to 2 s. The regions of PEG-DA exposed to UV light underwent free-radical polymerization and became cross-linked, while unexposed regions were dissolved in DI water after 5 min of development. The height of the resultant hydrogel microstructures varied from 2 to 5 μm , as measured with a Dektak³ surface profiler (Veeco Instruments, Santa Barbara, CA). Hydrogel microstructures for high-density cell patterning consisted of either an 80 \times 80 array of wells with individual well dimensions of 30 \times 30 μm and 20- μm walls or a 100 \times 100 microwell array with 20 \times 20 μm well dimensions and 20- μm walls.

High-resolution images of the hydrogel microstructures were obtained using a JSM 5600LV scanning electron microscopy (SEM) microscope (JEOL, Inc., Peabody, MA) operating at 10 mV of accelerating voltage. To avoid charging effects, substrates were sputter-coated with gold-palladium to a thickness of 10 nm prior to the SEM experiments. The same protocol was followed for the preparation and imaging of samples containing fixed mammalian cells and PEG microstructures without the cells.

Deposition of Collagen and Surface Characterization.

In the protein immobilization experiments, glass surfaces were treated with silane agent **2** containing secondary amines and patterned with PEG hydrogel, as described above. Samples were then placed into a 0.1 mg/mL solution of collagen (type I) in PBS (pH 7.4) for 1 h. Protein-modified surfaces were rinsed with DI water at least three times and stored at 4 $^{\circ}\text{C}$. Deposited collagen was characterized according to the procedures described below.

Protein immobilization within the PEG microwell patterns was visualized by means of fluorescence microscopy. Fluorescein-labeled collagen immobilized on the surface was imaged using a Nikon Eclipse TE2000 inverted microscope (Nikon, Japan) with an attached SPOT digital camera (Diagnostic Instruments, Inc., Burlingame, CA) at magnifications of 200 \times and 400 \times using fluorescein excitation/emission filters with wavelengths of 480 \pm 30 nm/535 \pm 40 nm.

Further characterization of the collagen-modified PEG microwells was performed by AFM. A Nanoscope III instrument (Digital Instruments, Santa Barbara, CA) operating in the tapping mode, with a standard 117- μm silicon cantilever, was

employed. All measurements were performed at room temperature in air. For the roughness determination, a 1 \times 1 μm region of the sample was scanned at 2 Hz. The root-mean-square (RMS) roughness of an acquired image was determined using Nanoscope III image analysis software and represented the average roughness of at least three smaller (0.25 \times 0.25 μm) regions. The number of AFM measurements to determine the RMS roughness was $n \geq 3$. Larger regions of the pattern were scanned at rates ranging from 0.2 to 0.5 Hz.

Cell Patterning. Murine 3T3 fibroblasts were cultured in 175-cm² tissue culture flasks at 37 $^{\circ}\text{C}$ in a humidified atmosphere with 10% CO₂/90% air. Fibroblasts were incubated in DMEM supplemented with 110 mg/L sodium pyruvate, 10% bovine calf serum, 200 U/mL penicillin, and 200 $\mu\text{g}/\text{mL}$ streptomycin. Cells were grown to confluence and passaged by trypsinization in a 0.05% trypsin/0.01% EDTA solution in PBS for 5 min at 37 $^{\circ}\text{C}$. The cell suspension was diluted 1:1 with a fibroblast culture medium and centrifuged at 800 rpm for 5 min. After aspiration of the supernatant, cells were reconstituted in a fresh fibroblast culture medium and counted using a hemocytometer. Fibroblast viability was typically better than 95%, as determined by trypan blue exclusion.

Rat hepatocytes were isolated and purified according to established protocols.³² Typically, 200–300 million cells were isolated from a single animal, with cell viabilities ranging between 85 and 95%, as established by trypan blue staining. The hepatocyte culture medium was composed of DMEM supplemented with 10% fetal bovine serum, 200 U/mL penicillin, 200 $\mu\text{g}/\text{mL}$ streptomycin, 7.5 $\mu\text{g}/\text{mL}$ hydrocortisone, 20 ng/mL epidermal growth factor, 14 ng/mL glucagon, and 0.5 U/mL insulin. For the cell-seeding experiments, glass slides, micropatterned with PEG, were cut into 25 \times 25 mm pieces and placed into 35-mm-diameter Petri dishes. Prior to cell seeding, samples were sterilized overnight in 70% ethanol and rinsed in DI water. When seeding the fibroblasts, 2 mL of the cell suspension at 1 \times 10⁶ cells/mL in the growth medium with 10% calf serum was introduced into the Petri dishes containing micropatterned glass templates. Cells incubated with patterned surfaces for 2 h at 37 $^{\circ}\text{C}$ were shaken every 30 min to help improve the seeding efficiency. After the 2-h incubation, the growth medium with unattached fibroblasts was aspirated out and replaced with 2 mL of fresh media. Fibroblasts patterned within PEG microwells were incubated at 37 $^{\circ}\text{C}$ for 12 h after the cell seeding and then fixed in 1% (v/v) glutaraldehyde in PBS for 30 min.

Studies were conducted to define the cell concentration leading to the highest efficiency of seeding of the cell array. Arrays of 80 \times 80 PEG microwells patterned on 25 \times 25 mm glass samples were placed into 35-mm-diameter Petri dishes and exposed to 2 mL of the cell suspension. Each glass slide typically contained two micropatterned regions occupying total of 32 mm². In the experiments conducted in parallel, patterned templates were exposed to cell concentrations ranging from 0.25 to 1 \times 10⁶ cells/mL. Samples were incubated with the cell suspension for 4 h with periodic shaking (every 15 min for the first hour) and fixed according to the protocol described above. Cell occupancy in the randomly selected region of the array comprised of \sim 400 wells was enumerated by manual counts at 100 \times magnification.

The cell occupancy was defined as

$$\text{cell occupancy (\%)} = \left(\frac{\text{no. wells occupied}}{\text{no. wells total}} \right) \times 100$$

For the same array of 400 wells, the number of contacts between cells residing in adjacent wells was noted. Cell contact was defined as the breach of any of the four PEG walls of the well that led to physical communication with cells in adjacent wells. For all the studies, the number of samples (n) was ≥ 4 .

Hepatocyte seeding was performed immediately after the isolation to ensure cell viability. Sterilized, PEG-patterned substrates were placed in 35-mm-diameter Petri dishes and exposed to 2 mL of hepatocyte suspension at the concentration of 5 \times 10⁵ cells/mL. After 2 h of incubation at 37 $^{\circ}\text{C}$, hepatocyte media with unattached cells was aspirated and replaced with 2 mL of fresh media. Patterned hepatocytes were incubated for 24 h at 37 $^{\circ}\text{C}$ and fixed according to the protocol described above.

The Live/Dead staining procedure for determining the viability of the patterned cells was followed in accordance with the manufacturer's instructions.³³ Stained cells were observed through fluorescein (480 ± 30 nm/ 535 ± 40 nm) and rhodamine (540 ± 25 nm/ 605 ± 50 nm) excitation/emission filters of a Nikon Eclipse inverted microscope. A Zeiss LSM 5 Pascal confocal microscope (Carl Zeiss, Inc., Thornwood, NY) was employed to collect composite, fluorescence, and brightfield images of the stained cells.

Results and Discussion

The ability to arrange cells on the surface in a controlled manner is of great importance for tissue engineering, high-throughput screening, and clinical diagnostics. The present publication utilized PEG hydrogel photolithography for creating microdomains with cell-repellent and cell-adhesive properties. The specificity of the cell–substrate interaction was further enhanced by selective immobilization of collagen in the glass regions defined by PEG micropatterns. The proposed surface-modification method enabled the formation of high-density arrays of 3T3 fibroblasts and primary rat hepatocytes.

Silane Modification of Glass Substrates. Assembly of silane coupling agents has proven crucial in ensuring the attachment of hydrogel microstructures to glass substrata. In general, silane adhesion promoters are used extensively in industry to ensure the integrity of the polymer/glass interface.³⁴ These adhesion promoters have also enabled the covalent linkage of hydrogels to silicon dioxide surfaces.^{35,36} In the present study, the self-assembly of alkoxy- and chlorosilanes was employed to introduce terminal acrylate and vinyl functional groups capable of taking part in the photoinitiated free-radical polymerization and covalently anchoring hydrogel microstructures to the glass substrate.

Fabrication of Hydrogel Micropatterns. The patterning of PEG hydrogel microstructures proceeded according to the steps outlined in Figure 1. The precursor solution containing photoinitiator and PEG-DA was spin-coated onto 75×25 mm silane-treated glass slides, forming a uniform layer. Spin-coating is a proven method for evenly distributing polymeric material over large surface areas; thus, much larger substrates could be seamlessly integrated into the process.

Glass slides coated with the PEG precursor solution were exposed to UV light through a photomask containing the desired features. Because each PEG-DA molecule contains two reactive C=C centers, propagation resulted in the localized formation of a highly cross-linked hydrogel. Similarly, the reaction between acrylate groups in the bulk and vinyl or acrylate moieties of the alkylsilanes self-assembled on the surface resulted in covalent anchoring of the hydrogel microstructures to the surface. Polymerization of the precursor polymer films containing 1% (w/v) photoinitiator occurred after 1–2 s of exposure to a collimated 365-nm UV source operating at 15 mW/cm². Unexposed regions of the precursor solution were developed in water, leaving behind surface-bound hydrogel micropatterns. Because of the water development, PEG hydrogel microstructures became hydrated and swollen. Despite drying with nitrogen and air following the development, the micropatterns were expected to retain

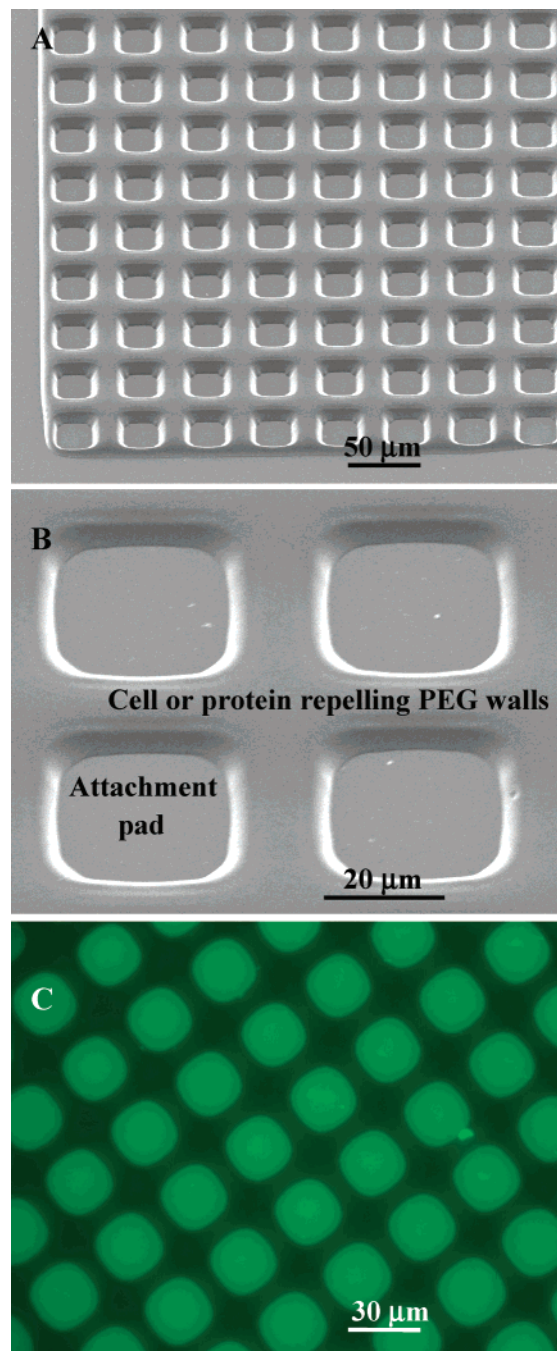


Figure 2. Micrographs of PEG microwells on glass. (A) SEM image of the high-density array of 30×30 μm hydrogel microwells with 20 - μm cell-resistant PEG side walls ($\times 270$). (B) Higher-magnification ($\times 900$) SEM micrograph of the hydrogel microstructures. (C) Fluorescein-labeled collagen coating the bottom of 30×30 μm wells ($\times 400$).

water. Previous study ascertained that a nearly 30% change in the height due to hydration occurred in microstructures fabricated from PEG-DA (MW 575).²⁸ Therefore, profilometry measurements conducted under ambient conditions reflect dimensions of the hydrated PEG gel. On the other hand, electron microscopy performed in high-vacuum conditions demonstrates PEG microstructures in the dehydrated state.

SEM micrographs of PEG microstructures fabricated in the microwell pattern are shown in Figure 2A,B. The pattern of square 30×30 μm wells with 20 - μm walls presented in Figure 2A enables a feature density of 400 wells/mm², or 7.5×10^5 wells for a 75×25 mm glass slide.

(33) *Handbook of Fluorescent Probes and Research Chemicals*, 6th ed.; Molecular Probes: Eugene, OR, 1996.

(34) Plueddemann, E. P. *Silane coupling agents*; Plenum Press: New York, 1982.

(35) van den Berg, A.; Bergveld, P.; Reinhoudt, D. N.; Sudholter, E. J. R. *Sens. Actuators* **1985**, *8*, 129–148.

(36) Lesho, M. J.; Sheppard, N. F. *Sens. Actuators, B* **1996**, *37*, 61–68.

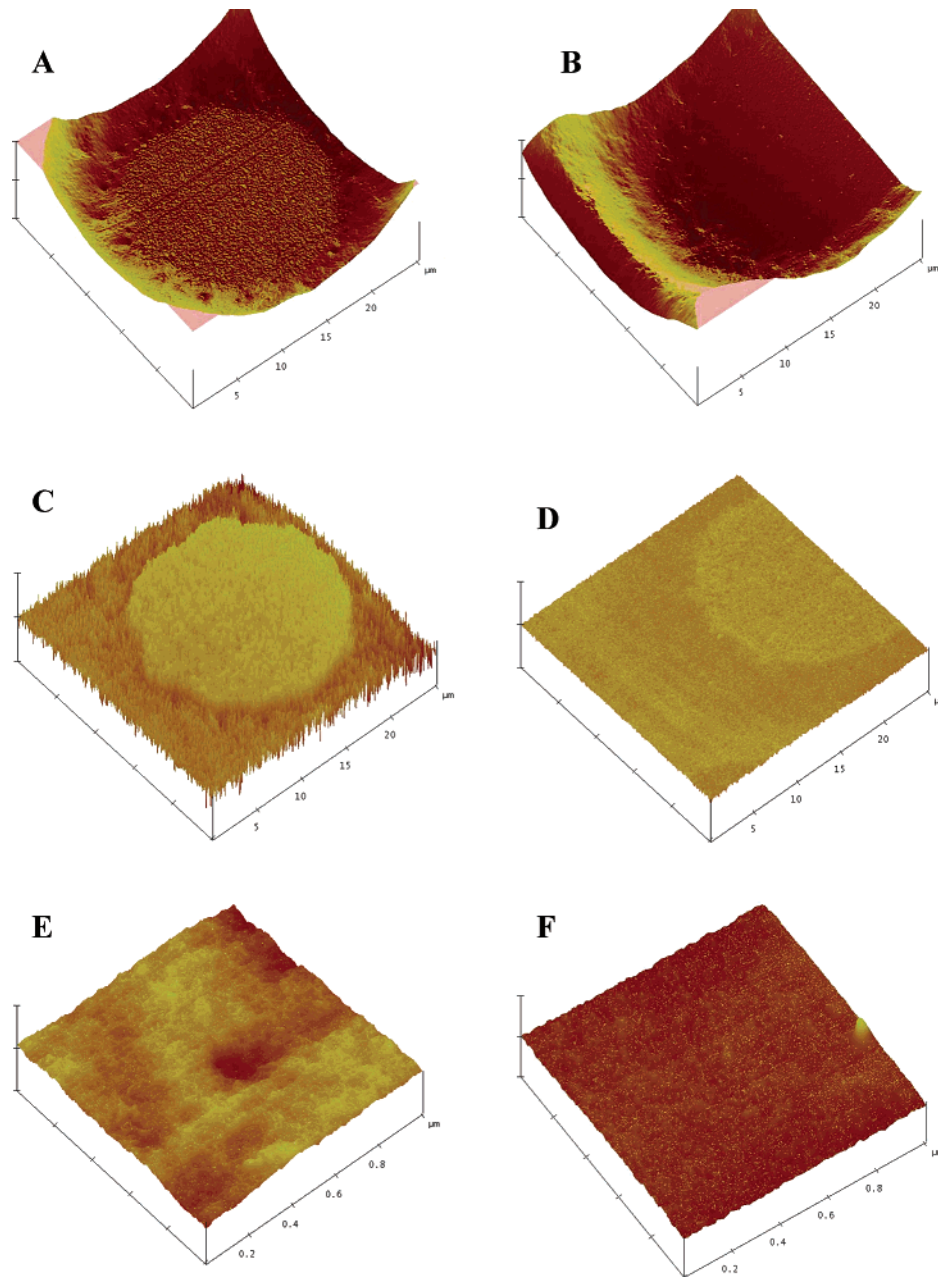


Figure 3. Height and phase-contrast AFM imaging of individual $400\text{-}\mu\text{m}^2$ wells with and without collagen. The following parameters were used to acquire and process the images for parts A–D: scan size of $25 \times 25 \mu\text{m}$, frequency 0.2 Hz, z scale 600 nm (height), and 50° (phase). Topographs for the RMS roughness determination presented in parts E and F were obtained by scanning a $1 \times 1 \mu\text{m}$ area inside individual wells at a 2-Hz frequency. Both images are presented with a z scale of 30 nm. (A) Height image of an individual collagen-coated well. (B) Microwell without collagen imaged in the height mode. (C) Phase-contrast image of the microwell with collagen. (D) Microwell without collagen imaged in the phase-contrast mode. (E) Collagen-coated surface. (F) Alkylsilane-modified glass surface without collagen.

This dense pattern modulates surface properties by creating defined cell-repelling and -adhesive regions, as illustrated by Figure 2B.

The heights of the fabricated hydrogel features ranged from 2 to $5 \mu\text{m}$, as measured by the profilometer. Individual well dimensions were chosen on the basis of the size of mammalian cells and do not represent the limit of the microfabrication process. A minimum feature size of $5 \mu\text{m}$ has previously been demonstrated.²⁸ Exposures were performed in the proximity mode with a separation gap of $100\text{--}150 \mu\text{m}$ between the photomask and the substrate. Thus, the rounded features of the PEG microstructures seen in Figure 2 may be explained as artifacts of light diffraction. Because the minimum feature size is propor-

tional to the square root of the separation gap,³⁷ fabrication of higher-resolution (single micrometer) PEG patterns with well-defined features requires contact lithography.

Protein Deposition and Surface Characterization

Interactions of epithelial cells with extracellular matrix (ECM) components play a major role in inducing and maintaining cell function. Specifically, primary hepatocytes cultured in vitro on type I collagen presented in two- or three-dimensional configurations have been shown to maintain liver-specific function and polarity.³⁸ Thus, to

(37) Ghandhi, S. K. *VLSI Fabrication Principles*, 2nd ed.; John Wiley & Sons: New York, 1994.

(38) Moghe, P. V.; Berthiaume, F.; Ezzell, R. M.; Toner, M.; Tompkins, R. G.; Yarmush, M. L. *Biomaterials* **1996**, *17*, 373–386.

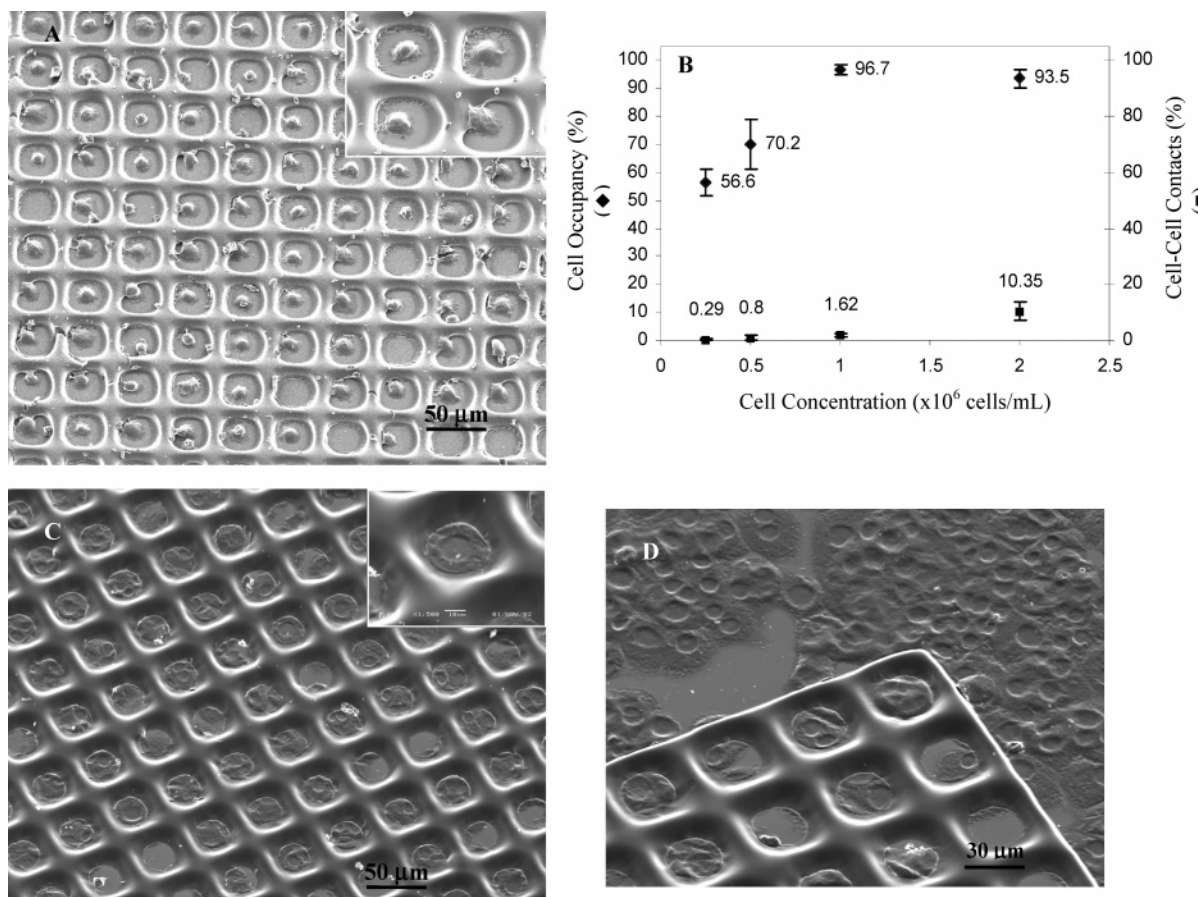


Figure 4. Patterning of 3T3 fibroblasts and primary rat hepatocytes in $30 \times 30 \mu\text{m}$ PEG wells. (A) 10×9 array of single fibroblasts with 91% cell occupancy ($\times 150$). The inset shows a higher-magnification image of confined fibroblasts ($\times 1200$). (B) Effects of the fibroblast concentration in solution on the occupancy of PEG microwells. Cell occupancy and cell–cell contact results are based on manual counts of the cells in ~ 400 wells; for all data points, $n \geq 4$. (C) High-density array of hepatocytes with one to three cells per well ($\times 250$); the inset shows individual hepatocytes ($\times 1500$). (D) Interface between the region with PEG-defined attachment sites and unpatterned, collagen-coated glass ($\times 370$).

engineer specific hepatocyte–surface interactions, PEG-patterned surfaces were modified with collagen. Because of the protein-resistant properties of PEG, localization of this ECM component within individual wells was expected.

To immobilize collagen, additional consideration in the selection of silane adhesion promoters was given to routes for the conjugation of proteins on glass. These routes can involve covalent binding³⁹ or electrostatic assembly.⁴⁰ Thus, a surface coupling agent should contain pendant C=C bonds for anchoring the hydrogel microstructures and reactive or protonatable moieties for binding to proteins. Because surface modification agents containing C=C and protein-reactive (e.g., primary amines) functional groups were not commercially available, the silane coupling agent **2** with pendant protonatable secondary amine groups was chosen. Glass slides, chemically modified with **2**, were micropatterned with PEG and immersed in a 0.1 mg/mL collagen solution in pH 7.4 PBS. The amine-containing silane molecules imparted a positive charge on the surface, whereas collagen was partially deprotonated (negatively charged) under neutral deposition conditions (pH 7.4) as a result of its relatively low isoelectric point (pI) of 5.5.⁴¹ Thus, interactions of charged protein molecules with an oppositely charged substratum resulted in the surface immobilization of collagen.

Figure 2C demonstrates results of a representative experiment where fluorescent labeling was used to visualize the localization and patterning of collagen. Green fluorescent regions correspond to the glass attachment pads at the bottom of the $30 \times 30 \mu\text{m}$ wells where fluorescein-conjugated collagen deposited, while the dark regions correspond to the protein-repelling PEG walls of the microwells. As indicated by these results, collagen deposited selectively on the glass attachment pads of the PEG-micropatterned surface.

AFM analysis of the PEG pattern, demonstrated in Figure 3, was employed to ascertain the localization of protein within individual wells. AFM cantilever geometry permitted a maximum z range of $6 \mu\text{m}$; thus, hydrogel features with heights below the maximum could be imaged. Figure 3A presents a surface plot of a $20 \times 20 \mu\text{m}$ hydrogel well with collagen deposited at the bottom while Figure 3B illustrates analysis of a similar well without collagen. In both cases, craterlike wells have smooth PEG walls; however, the attachment pad of the collagen-coated well appears much rougher than that of the control sample. The differences in the material properties of the PEG walls and the collagen-coated bottom of the well are accentuated by the phase-contrast AFM images presented in Figure 3C,D. While the height imaging mode refers to the amplitude of oscillation of the AFM cantilever, phase-contrast imaging monitors the phase lag of the sinusoidal oscillation due to cantilever–surface interactions.⁴² Be-

(39) Hermanson, G. T. *Bioconjugate Techniques*; Academic Press: New York, 1996.

(40) Decher, G. *Science* **1997**, *227*, 1232–1237.

(41) Luescher, M.; Ruegg, M.; Schindler, P. *Biopolymers* **1974**, *13*, 2489–2503.

(42) Garcia, R.; Perez, R. *Surf. Sci. Rep.* **2002**, *47*, 197–301.

cause of its sensitivity toward materials-induced effects, phase imaging has been used widely for characterization of surface composition, including visualization of proteins on rough substrates.^{43,44} The phase-contrast image of the well presented in Figure 3C shows a clearly demarcated protein region corresponding to the dimensions of the attachment pad. A similar distinct boundary is lacking in the well that was not modified with collagen, as seen in Figure 3D.

AFM analysis of smaller areas ($1 \mu\text{m}^2$) was employed to investigate substratum topology within the hydrogel microwells. Figure 3E,F demonstrates representative AFM images of the surface with and without collagen. Surfaces containing adsorbed protein had a RMS roughness of $1.13 \pm 0.03 \text{ nm}$, as compared to $0.7 \pm 0.04 \text{ nm}$ for the substrata modified with only the alkylsilane. An increased surface roughness is logical given the deposition of large (300 kDa),⁴⁵ rod-shaped collagen molecules onto fairly smooth, alkylsilane-coated substrata. Similar changes in the surface properties due to collagen deposition have been reported in the literature.⁴⁶

Overall, AFM analysis of the surfaces containing adsorbed collagen showed a distinct PEG–collagen interface, verified protein immobilization on the glass attachment pads, and yielded little evidence of protein adsorption on the PEG microstructures. One has to note that we have not yet characterized the elemental composition of the surface to identify any residual PEG in the attachment pads of the microwells. However, AFM analysis of the surface inside the microwells did not reveal any topographical evidence of such residues.

Cell Patterning. Controlling the attachment of 3T3 fibroblasts and primary hepatocytes presented a set of interesting challenges. Fibroblasts are robust cells that adhere indiscriminately to a variety of surfaces by attaching to their own secreted ECM proteins. On the other hand, primary hepatocytes exhibit more selective behavior in vitro, preferentially attaching and differentiating on surfaces containing collagen.^{38,47} Thus, the method presented here had to combine excellent overall resistance to cell adhesion with the flexibility of designing specific cell–surface interactions.

Figure 4 demonstrates results of the fibroblast and hepatocyte patterning. The cells adhered almost exclusively to the attachment pads defined by the PEG microfabrication method. This behavior was reproducible and occurred on the large scale, as shown in Figure 4A where an array of 90 wells were 91% occupied by fibroblasts, with most wells containing single cells. Higher-magnification SEM micrographs (inset of Figure 4A) further illustrate the confinement of fibroblasts within the three-dimensional microfabricated PEG wells.

Cell occupancy of the microwells was investigated as a function of the fibroblast concentration to establish a robust and reproducible cell-seeding protocol. In these experiments, PEG-micropatterned glass surfaces were exposed to varying fibroblast concentrations, incubated for 4 h, and fixed in accordance to the protocols described in the Experimental Section. Assessment of the seeding efficiency was made on the basis of manual counts of the

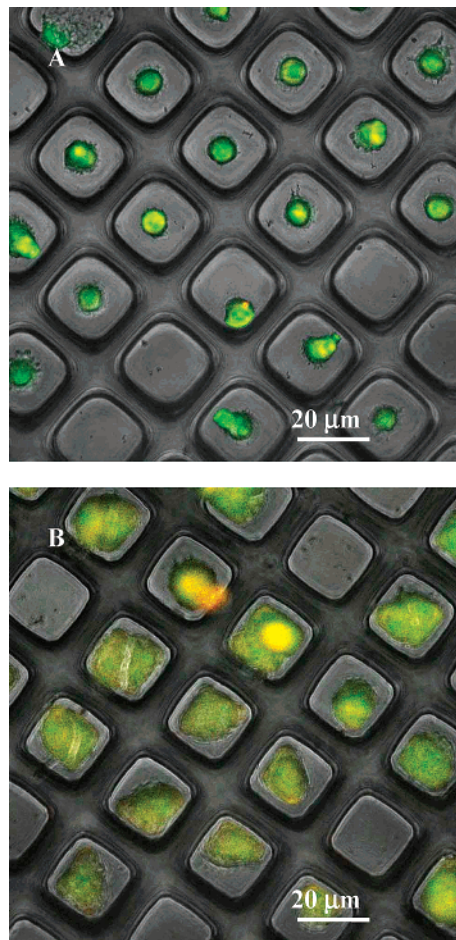


Figure 5. Viability of the cells confined within PEG microwells with $30 \times 30 \mu\text{m}$ individual dimensions as determined by the Live/Dead assay. Both micrographs were obtained at $\times 400$ using confocal microscopy. (A) 3T3 fibroblasts after 12 h of incubation. (B) Primary hepatocytes after 24 h of incubation.

cells occupying randomly selected regions of the array comprised of ~ 400 wells. Results of these experiments presented in Figure 4B illustrate the direct correlation between the cell concentration in solution and the quality of the high-density cell-array formation. The cell-seeding process was highly reproducible, as illustrated by a $96.7 \pm 1.9\%$ cell occupancy for the fibroblast concentration of 1×10^6 cells/mL. This concentration was an optimal cell-seeding parameter as a result of the combination of the high cell occupancy and the low cell cross-talk. Importantly, challenging PEG-patterned glass surfaces with the even higher cell concentration of 2×10^6 fibroblasts/mL did not improve the seeding efficiency. In fact, using a higher-than-needed cell concentration had deleterious effects because the number of contacts between cells confined in adjacent wells is increased from $1.62 \pm 0.68\%$ for the 1×10^6 cells/mL concentration to $10.35 \pm 3.5\%$ for the 2×10^6 cells/mL concentration.

Hepatocytes interacted specifically with collagen-modified attachment pads when exposed to PEG-micropatterned glass surfaces, adhering after 1 h and becoming fully confluent within individual wells after a 24-h incubation period. As seen from Figure 4C, cells attached preferentially inside the wells in a highly reproducible fashion, with individual $30 \times 30 \mu\text{m}$ wells containing one to three hepatocytes.

Figure 4D demonstrates the contrast between a confluent monolayer of hepatocytes formed on an unpatterned collagen-coated glass surface and the discrete groups of

(43) Holland, N. B.; Marchant, R. E. *J. Biomed. Mater. Res.* **2000**, *51*, 307–315.

(44) Cacciafesta, P.; Hallam, K. R.; Watkinson, A. C.; Allen, G. C.; Miles, M. J.; Jandt, K. D. *Surf. Sci. Rep.* **2001**, *491*, 405–420.

(45) Mertig, M.; Thiele, U.; Bradt, J.; Liebig, G.; Pompe, W.; Wendrock, H. *Surf. Interface Anal.* **1997**, *25*, 514–521.

(46) Denis, F. A.; Hanarp, P.; Sutherland, D. S.; Gold, J.; Mustin, C.; Rouxhet, P. G.; Dufrene, Y. F. *Langmuir* **2002**, *18*, 819–822.

(47) Berthiaume, F.; Moghe, P. V.; Toner, M.; Yarmush, M. L. *FASEB J.* **1996**, *10*, 1471–1484.

cells, residing within PEG compartments and lacking communication with neighboring units. While illuminating cell-resistant properties of the PEG microstructures, this image underscores the potential utility of this method for defining and designing cell–cell interactions. Such interactions have recently been implicated by Nelson and Chen as important modulators of cell function.⁴⁸ In their study, micromolded agarose structures were employed to engineer intercellular communications to observe changes in proliferation rates.

It is also interesting to note that, despite conforming to the shape of the wells, hepatocytes within and without the patterns exhibited a planar, extended morphology, as illustrated by Figure 4D. The substratum composition is a central factor in defining the cytoskeletal arrangement of the hepatocytes,^{38,47} and the morphology presented here is consistent with cells demonstrating affinity toward the surface. Similar behavior was not observed when hepatocytes were challenged with micropatterned substrates lacking collagen. In fact, hepatocytes were not able to attach to such surfaces within the 1-h incubation time allotted for cell–surface interactions.

The viability of the patterned cells was determined by Live/Dead fluorescence staining. To validate cell viability as a function of the spatial position, images of the patterned, stained cells were collected simultaneously in the fluorescein, rhodamine, and brightfield channels of the confocal microscope. This resulted in the creation of composite images illustrating the location of the fluorescing cells within PEG microwells (seen in Figure 5). Both cell types remained viable, as indicated by the predominance of green fluorescence emission. Figure 5A demonstrates a representative array of viable, single fibroblasts observed after 12 h of incubation. While remaining viable, these cells were unable to spread and were situated in the middle of the attachment site. Nonviable fibroblasts, not shown in this micrograph but observed in the course of the experiments, were normally deposited on the cell-repellent walls of the hydrogel microwells. Unlike fibroblasts, viable hepatocytes, imaged in Figure 5B after 24

h of incubation, became confluent and assumed the shapes of the confining PEG microstructures. Nonviable hepatocytes in the same figure appear rounded and were unable to adhere to the collagen-presenting attachment sites occupied by other cells. Overall, Live/Dead staining pointed to the viability of micropatterned mammalian cells employed in the study.

Conclusions

The present paper outlines a microfabrication-derived method for precisely controlling cell–surface interactions. PEG was photopatterned to manufacture high-density arrays of hydrogel microwells on glass, creating a highly ordered surface with defined cell-repellent and cell-adhesive properties. Selective ECM protein deposition was employed to engineer attachment sites within the micropatterns for specific cell–substratum interactions. Successful high-density patterning of 3T3 fibroblasts and primary hepatocytes within PEG microstructures was demonstrated. The general strategy for cell patterning presented in this manuscript can be employed in tissue engineering to study specific cell–cell interactions. It is also highly applicable for high-throughput screening and clinical diagnostics, as well as interfacing cellular and microfabricated components of biomedical microsystems.

Acknowledgment. We would like to thank Drs. Daniel Irimia and Arno W. Tilles for critically reviewing the manuscript. Technical assistance and helpful comments provided by Nicholas Telischak and Octavio Hurtado are greatly appreciated. AFM studies were conducted at the Center for Materials Science and Engineering at MIT with the assistance of Ms. Elizabeth Shaw. SEM was performed at the W. M. Keck Microscopy Facility at the Whitehead Institute for Biomedical Engineering. Confocal microscopy was performed at CNY-6 Confocal Microscopy Core at MGH with assistance from Mr. Igor Bagayev. This study was supported by National Institutes of Health (Grant T32GM07035).

LA035129B

(48) Nelson, C. M.; Chen, C. S. *FEBS Lett.* **2002**, *514*, 238–242.